PROCEEDINGS OF SCIENCE

Experimental overview of EFT measurements in the electroweak sector based on the results of the ATLAS and CMS experiments

Evgeny Soldatov*, **on behalf of the ATLAS and CMS Collaborations**[a,∗]

[a] *National Research Nuclear University «MEPhI», Kashirskoe shosse 31, Moscow, Russia*

E-mail: EYSoldatov@mephi.ru

The report contains an overview of the current experimental results from ATLAS and CMS collaborations at LHC interpreted in terms of the effective field theory. A set of reviews of the individual analyses is given. Diboson final states are considered, as well as the recent ATLAS EFT combination of several SM analyses. The main problems of the EFT interpretations are highlighted.

The Tenth Annual Conference on Large Hadron Collider Physics - LHCP2022
16-20 May 2022
online

*The work of Evgeny Soldatov is supported by the Ministry of Science and Higher Education of the Russian Federation, Project No 0723-2020-0041

∗Speaker

PoS(LHCP2022)178

1. Introduction and theoretical framework

After the discovery of Higgs boson in 2012 [1, 2] the activities dedicated to the search of any deviations from Standard Model (SM) have been largely intensified. Today, 10 years later, still no success in direct search of any beyond Standard Model (BSM) physics effects in ATLAS [3] and CMS [4] experiments at the LHC was reached [5].

Growing integrated luminosity without an increase of the collision energy strongly motivates indirect BSM (or new physics) search. This type of search allows the study of inaccessible kinematic regions in energy based on low-energetic effects, e.g. anomalous triple/quartic gauge couplings (aTGCs/aQGCs). Effective field theory (EFT) is a model independent approach to parameterize BSM effects in the Lagrangian using operators with mass dimension greater than four. Constants of these operators C, so-called Wilson coefficients, can be measured or constrained using experimental data. Such constraints can be then extrapolated to the parameters of the concrete BSM model.

Operators used in EFT are gauge invariant combinations of SM fields. A popular basis of dimension-6 operators is the Warsaw basis [6]. It reduces the number of operators from 2499 to 59. These operators are used for the description of aTGCs in the diboson final states W+any other electroweak boson and in the vector boson fusion (VBF) final states of single bosons W and Z. Neutral aTGCs can be described by four operators of dimension-8, O_{BW}, O_{BB}, O_{WW} and $O_{\mathrm{B\tilde{W}}}$ from [7]. Finally, aQGCs in EFT are described by dimension-8 operators detailed in [8].

The full amplitude is the sum of SM and BSM contributions, while the combined cross-section is proportional to the squared amplitude. Thus in case of one non-zero BSM operator there are 3 terms: SM term, interference (or linear) term and fully BSM quadratic term. The last term has suppression order of the Λ^{-4}, where Λ is the characteristic mass scale of new physics. However it should be noted that the interference terms from dimension-8 operator also have order of the Λ^{-4}. This means that the validity of any derived constraints using both linear and quadratic terms (full model) is limited by the unknown effect of the leading dimension-8 contributions. From the other side if one drops the quadratic term, the limits become much weaker, since the interference term can be highly suppressed due to different helicity configurations for the SM and BSM components.

2. ATLAS EFT combination

The combined EFT interpretation includes WW, WZ, $4l$ and VBF Z final states [9]. The first two analyses use the partial Run2 dataset of 36 fb^{-1} of data and the second two use the full Run2 dataset of 139 fb^{-1}. Several different distributions are used for limit setting procedure: $p_T^{\mathrm{lead.lep}}$ for WW, m_{T}^{WZ} for WZ, m_{4l} for $4l$ and ϕ_{jj}[1] for VBF Z. The combined likelihood function accounts for experimental uncertainties and correlation as well as theory uncertainties. Results are provided for a linear and full model separately, see Figure 1. Since the measurements contain insufficient information to constrain all coefficients simultaneously, one uses a modified Warsaw basis of linear combinations of operators in this analysis.

[1] $p_T^{\mathrm{lead.lep}}$ - transverse momentum of the leading jet in the event; transverse mass $m_{\mathrm{T}}^{WZ} = \sqrt{(\sum p_T^{\ell} + E_T^{miss})^2 - (\sum \vec{p}_T^{\,\ell} + \vec{E}_T^{miss})^2}$, where $\vec{p}_T^{\,\ell}$ and p_T^{ℓ} are the charged lepton transverse momentum vectors and their magnitude, respectively, and $\vec{E}_T^{miss}$ and $\vec{E}_T^{miss}$ are the missing transverse momentum vector and its magnitude; m_{4l} - invariant mass of 4 charged leptons; ϕ_{jj} - azimuthal angle between leading and subleding jet.

PoS(LHCP2022)178

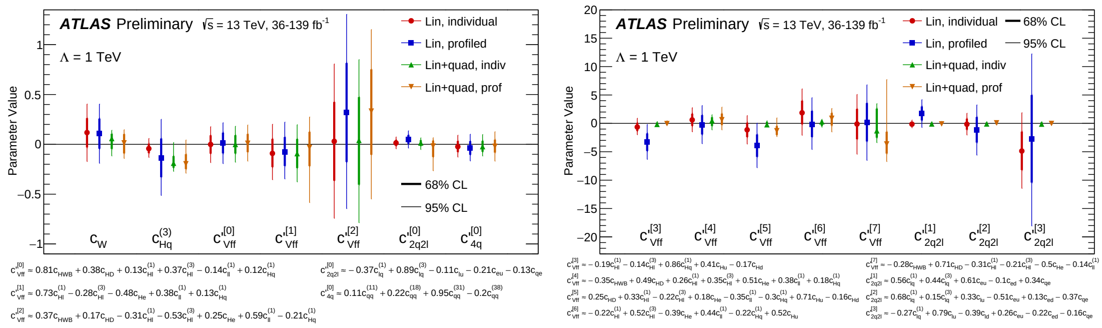

Figure 1: Confidence intervals for the 15 parameters included in the combined maximum likelihood fit. Results are quoted both for fits linear in the parameters and for fits that take into account also quadratic contributions. Comparisons of the two results can be used to estimate uncertainties due to the truncation of the EFT expansion [9].

The combination is sensitive to 33 operators in total. Limits are set for 13 linear combinations and 2 individual operators. The full model limits are significantly better than the linear ones. It indicates a possible invalidity of the truncated EFT expansion. All measurements agree with the SM expectation at the level of about two standard deviations or better.

3. Individual analyses sensitive to aTGCs

The $W\gamma$ final state is measured by CMS using the full Run2 dataset. The first analysis uses p_T^γ distribution for setting the limits on 4 dimension-6 operators O_{WWW}, O_{B}, $O_{\tilde{\mathrm{W}}}$ and $O_{\mathrm{W\tilde{W}W}}$ [10].

The second analysis uses the photon momentum, p_T^γ, and the azimuthal angle ϕ of the lepton in a center-of-mass frame of the $W\gamma$ system for the limit setting procedure [11]. A different helicity configuration for the SM and BSM components suppresses the interference part only when considering observables inclusive over the decay angles. In the case of taking the azimuthal angle into account, the sensitivity to interference increases, which is of order of Λ^{-2}. Linear-term-only and full model cases are investigated for the operator O_{WWW} and shown in the left part of Figure 2.

The WW + jets analysis from ATLAS uses the full Run2 dataset [12] and the differential cross-section is measured. The unfolded $m_{e\mu}$ distribution is used for the aTGC study, where the O_{W} EFT operator is probed. The limits are obtained for linear-only and full model cases. To overcome the suppression of the interference term, the presence of at least one highly boosted jet is required (Figure 2, right).

The WZ final state analysis by CMS uses the m_{WZ} distribution for setting the limits on 3 CP-conserving (O_{WWW}, O_{W} and O_{b}) and 2 CP-violating operators ($\tilde{O}_{\mathrm{WWW}}$ and $\tilde{O}_{\mathrm{W}}$) [13]. The limits are obtained for linear-only and full model cases. The EFT approach cannot be used at any arbitrary energy, because this leads to a breaking of the unitarity. To overcome this problem, one should set the limits with an application of some energy cutoff preventing the infinite growth of the cross-section. A scan of the limits versus several cutoff scales (Figure 3) is performed for all considered operators.

The 4l final state (l = e, μ) analyses by ATLAS and CMS are performed using the full Run2 dataset. The CMS analysis uses the m_{ZZ} distribution to perform a BSM neutral TGC

PoS(LHCP2022)178

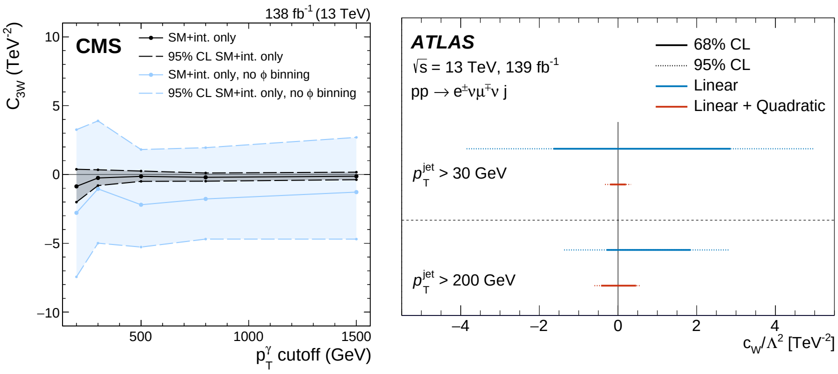

Figure 2: The 95% CL confidence intervals for $C_{3\mathrm{W}}$ as a function of the maximum p_{T}^{γ} bin included in the fit (left). The binning in ϕ is (not) used for black (blue) limits [10]. Confidence level intervals from a fit of the unfolded $m_{e\mu}$ distribution for both $p_{\mathrm{T}}^{\mathrm{lead.jet}} > 30$ GeV and $p_{\mathrm{T}}^{\mathrm{lead.jet}} > 200$ GeV (right). Linear fit results are shown in blue and fits for which terms linear and quadratic in C_{W} are included are shown in red [12].

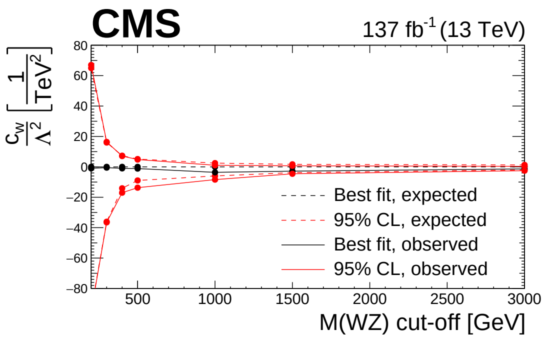

Figure 3: Observed and expected evolution of the confidence intervals in the C_{W}/Λ^2 EFT anomalous coupling parameter in terms of the cutoff scale given by different restrictions in the M_{WZ} variable [13].

interpretation [14]. The aTGC is interpreted using the old vertex functions formalism, which still remains more complete than EFT for neutral TGCs [7, 15]. The obtained limits are recalculated into the dimension-8 EFT formalism. The ATLAS analysis uses all production channels of the $4l$ final state [16], and 22 out of 59 operators from the Warsaw basis give sizable contribution to this final state. Different unfolded observables are used: m_{4l}, m_{34}, $\Delta\phi(l,l)$, $\Delta\phi(Z,Z)$. Two sets of limits are obtained: full model and linear only, detailed in [14, 16].

4. Individual analyses sensitive to aQGCs

Vector boson scattering processes are the main interest among all electroweak diagrams since they are sensitive to aQGCs, which are realized by EFT dimension-8 operators. The common signature is the presence of two high-energy jets that are well separated in rapidity.

Various final states were measured by CMS [17–20]. Leptonic decays of the bosons are used (only to e or μ) in these analyses. Distributions in m_{VV} are used to extract the limits on different operators from different analyses and results are complementary. Each analysis sets the strongest limits on several coefficients. Unitarity bounds are obtained in all analyses, however only one analysis [17] published the two sets of limits including unitarized ones.

5. Conclusions

EFT interpretations have become a standard part of many electroweak analyses nowadays. A number of final states involved in these activities is increasing. The main challenges come from the sizable correlation between the operators and from the unitarity preservation treatment as well as from the correct accounting for the higher dimension operator effects.

All results discussed here from the ATLAS and CMS experiments are compatible with the SM so far. Some interesting results from Run2 of the LHC are still on the way together with the new EFT combinations using Run3 data.

References

[1] ATLAS Collaboration, Phys. Lett. B **716** (2012) 1–29

[2] CMS Collaboration, Phys. Lett. B **716** (2012) 30–61

[3] ATLAS Collaboration, JINST **3** (2008) S08003

[4] CMS Collaboration, JINST **3** (2008) S08004

[5] A. Hinzmann, PoS **EPS-HEP2021** (2022) 035

[6] B. Grzadkowski et al., JHEP **10** (2010) 085

[7] C. Degrande et al., Annals Phys. **335** (2013) 21–32

[8] O. J. P. Eboli and M. C. Gonzalez-Garcia, Phys. Rev. D **93** (2016) 093013

[9] ATLAS Collaboration, ATL-PHYS-PUB-2021-022

[10] CMS Collaboration, Phys. Rev. Lett. **126** (2021) 252002

[11] CMS Collaboration, Phys. Rev. D **105** (2022) 052003

[12] ATLAS Collaboration, JHEP **06** (2021) 003

[13] CMS Collaboration, JHEP **07** (2022) 032

[14] CMS Collaboration, Eur. Phys. J. C **81** (2021) 200

[15] ATLAS Collaboration, JHEP **12** (2018) 010

[16] ATLAS Collaboration, JHEP **07** (2021) 005

[17] CMS Collaboration, Phys. Lett. B **809** (2020) 135710

[18] CMS Collaboration, Phys. Lett. B **811** (2020) 135988

[19] CMS Collaboration, Phys. Rev. D **104** (2021) 072001

[20] CMS Collaboration, Phys. Lett. B **812** (2020) 135992

PoS(LHCP2022)178